Composites: Part B 66 (2014) 328–339

Contents lists available at ScienceDirect

Composites: Part B

journal homepage: www.elsevier.com/locate/compositesb

Exact closed-form solution for non-local vibration and biaxial buckling of bonded multi-nanoplate system

Danilo Karličić [a], Sondipon Adhikari [b], Tony Murmu [c,*], Milan Cajić [a]

[a] Mathematical Institute of the SASA, Kneza Mihaila 36, 11001 Belgrade, Serbia
[b] College of Engineering, Swansea University, Singleton Park, Swansea SA2 8PP, UK
[c] School of Engineering, University of the West of Scotland, Paisley PA12BE, UK

ARTICLE INFO

Article history:
Received 12 February 2014
Received in revised form 2 May 2014
Accepted 28 May 2014
Available online 9 June 2014

Keywords:
A. Nano-structures
B. Vibration
C. Analytical modeling
Multi-nanoplate system

ABSTRACT

In recent years, nonlocal elasticity theory is widely used for the analytical and computational modeling of nanostructures. This theory, developed by Eringen, has shown to be practical for the vibration and buckling analysis of nanoscale structures and reliable for predesign procedures of nano-devices. This paper considers buckling and dynamic analysis of multi-nanoplate systems. This type of system can be relevant to composite structures embedded with graphene sheets. Exact solutions for the natural frequencies and buckling loads of multi-nanoplate systems have been proposed by considering that the multi-nanoplate system is embedded within an elastic medium. Nonlocal elasticity theory is utilized for the mathematical establishment of the system. The solutions of the homogenous system of differential equations are obtained using the Navier's method and trigonometric method. An asymptotic analysis is proposed to show the influence of increasing number of nanoplates in the system. Analytical expressions are validated with existing results in the literature for some special cases. Numerical results based on the analytical expressions is shown to quantify the effects of the change in nonlocal parameter, stiffness coefficients of the elastic mediums and the number of layers on the natural frequencies and buckling load.

© 2014 Elsevier Ltd. All rights reserved.

1. Introduction

In analogy to the plate structures widely used in macro-engineering practice, there are also two-dimensional structures on nano-scale level called nanoplates. These structures are synthetized from various types of new materials that makes graphene sheets [1–8], gold nanoplates [9–11], silver nanoplates [12–15], boron-nitride sheets [16–19] and ZnO nanoplates [20–22] and carbon nanotubes [23–25] that can be obtained by rolling the two-dimensional nanostructures into a tube. Due to the exceptional characteristics, nanoplates are convenient for possible application in nanoelectromechanical systems (NEMS), nanooptomechanical systems (NOMS), nanocomposites, nanosensors, nanoactuators and biomedical systems [26–30].

Many of the above mention types of single or multi-nanoplate systems, bounded with certain type of medium, can be theoretically modeled using the same phenomenological assumptions as in case of classical plate systems [31,32]. However, experimental investigations [33,34] and atomistic simulations [35] have shown that the small-scale effects in the analysis of mechanical properties of nanostructures cannot be neglected. Molecular dynamics simulation is convenient method to simulate the mechanical behavior of small size structures but it is computationally expensive for structures with large number of atoms. Thus, much effective approaches are one that uses methods of classical continuum mechanics with necessary modifications that considers the effects appearing at the nano-scale level. In papers, [36–39] authors have used continuum-based models of single and multi-layered graphene sheets taking into account van der Waals (vdW) interaction between sheets and using different potential models. Another way to consider small-scale effects and the atomic forces in analysis of nano-scale structures is to use the nonlocal elasticity theory of Eringen [40]. This theory is used in numerous studies of nanostrucures and it is often used for reliable and fast analysis.

The multi-nanoplate system considered in this paper is different from multi-layer or double-layer systems presented in [37–39,41]. This difference is reflected in the fact that mentioned multi-layer and double-layer systems are bonded by a constant vdW force while the multi-nanoplate systems are bonded by an elastic medium with certain stiffness. The system studied here is particularly relevant to the future generation graphene based composite

* Corresponding author. Tel.: +44 (0) 141 848 3235.
E-mail address: murmutony@gmail.com (T. Murmu).

http://dx.doi.org/10.1016/j.compositesb.2014.05.029
1359-8368/© 2014 Elsevier Ltd. All rights reserved.

materials. Nonlocal theory is widely used for theoretical investigation of mechanical properties of nanostructures. However, vibration and buckling analysis of nanoplates is performed in the limiting number of studies [42–56].

Complex nanoplate systems bonded by a certain type of medium are important from both practical and theoretical point of view. As reported in [11] uniform stress imposed by the polymer matrix causes the symmetric buckling of ultrathin gold nanoplates. Vibration properties of single and multi-layer graphene sheets as electromechanical resonators are reported in [5]. In addition, nanoplates can be used in nano-optomechanical system (NOMS) [57,58]. Graphene sheets, gold nanoplates or other type of nanoplates dispersed in polymer matrix are behaving as nanocomposites [59–63]. Thus, vibration and buckling analysis of these systems may be important for their potential application in nano-scale devices.

Important results on the vibration of a single, double and multilayer graphene sheets embedded in an elastic medium, with vdW forces considered, are those by Pradhan and Phadikar [64,65]. The natural frequencies are determined analytically for a single and double-layer graphene sheet systems, whereas for a multi-layer system the frequencies are determined numerically. Recently, Murmu and Adhikari [66] and Pouresmaeeli et al. [68] used the nonlocal theory for vibration analysis of double-nanoplate system bonded with elastic medium. For the same system, Murmu et al. [67] performed buckling analysis for the system under uniaxial compression and later in [69] for the system under biaxial compression. Extension of the previously mentioned work would be vibration and buckling analysis of these systems for arbitrary number of nanoplates.

In this paper, we consider such kind of contribution proposing the exact solution method for the free transverse vibration of multi-nanoplate system and for the buckling stability. The paper is done within the framework of Eringen's nonlocal elasticity and modifying the Kirchhoff's plate theory. Simply supported boundary conditions to all four ends of nanoplates are employed for two different "chain" conditions, "Clamped-Chain" and "Free-Chain". This paper presents the unique procedure to find the exact solution for natural frequencies and buckling load of elastically coupled multi-nanoplate system (MNPS) using the so-called trigonometric method. Results are validated for the special case of MNPS when two elastically coupled nanoplates are system with the results for double-nanoplate system presented in [66] for vibration and in [69] for buckling analysis. The paper examines the nonlocal scale effects, effects of higher modes, aspect ratio and various coupling springs on natural frequencies and buckling load of MNPS. This study may be useful for future investigations of other types of multi nano-structure systems.

2. Overview of nonlocal elasticity relations

The basic assumption in the nonlocal theory of elasticity is that the stress at a point is function of strains at all points of the elastic body. Based on this assumption, in [70] Eringen presented an integral form of constitutive relation for a nonlocal stress tensor. In addition, the small-scale effects are accounted by considering internal size effects as a material parameter. The integral form of the nonlocal constitutive relation for a three-dimensional homogenous elastic body is

$$\sigma_{ij}(\boldsymbol{x}) = \int \alpha(|x-x'|,\tau) C_{ijkl}\varepsilon_{kl}(x')dV(x'), \forall x \in V, \tag{1a}$$

$$\sigma_{ij,j} = 0, \tag{1b}$$

$$\varepsilon_{ij} = \frac{1}{2}(u_{i,j} + u_{j,i}), \tag{1c}$$

where C_{ijkl} is the elastic modulus tensor for classical isotropic elasticity; σ_{ij} and ε_{ij} are stress and strain tensors, respectively, and u_i is displacement vector. With $\alpha(|x-x'|,\tau)$ we denote the nonlocal modulus or attenuation function, which incorporates nonlocal effects into the constitutive equation at the reference point x produced by the local strain at the source x'. The above absolute value of difference $|x-x'|$ denotes the Euclidean metric. The parameter $\tau = (e_0\tilde{a})/l$ where l is the external characteristic length (crack length, wavelength), $\tilde{a}$ describes the internal characteristic length (lattice parameter, granular size and distance between bounds) and e_0 is a constant appropriate to each material that can be identified from atomistic simulations or by using the dispersive curve of the Born–Karman model of lattice dynamics. Eringen has introduced constant e_0 as equal to 0.39. In the general case, the value of $(e_0\tilde{a})$ is taken in range of 0–2[nm] [45]. In fact, the value of nonlocal parameter is quite scattered and its exact value depends on various parameters of a structure. However, due to difficulties arising in analytical analysis of continuum systems by using the constitutive equations in integral form, Eringen [40] has reformulated constitutive equations by its transformation to a differential form. Further, such form is proved as very effective, simple, and convenient for analytical analysis of nanostructured systems. The differential form of the nonlocal constitutive relation

$$\left(1-\mu\nabla^2\right)\sigma_{ij} = t_{ij}, \tag{2}$$

where ∇^2 is the Laplacian; $\mu = (e_0\tilde{a})^2$ is the nonlocal parameter; and $t_{ij} = C_{ijkl}\varepsilon_{kl}$ is the classical stress tensor. From Eq. (2), the constitutive relations for homogeneous elastic nanoplates can be expressed as

$$(1-\mu\nabla^2)\begin{pmatrix}\sigma_{xx}\\ \sigma_{yy}\\ \tau_{xy}\end{pmatrix} = \begin{bmatrix}\frac{E}{1-\vartheta^2} & \frac{\vartheta E}{1-\vartheta^2} & 0\\ \frac{\vartheta E}{1-\vartheta^2} & \frac{E}{1-\vartheta^2} & 0\\ 0 & 0 & G\end{bmatrix}\begin{pmatrix}\varepsilon_{xx}\\ \varepsilon_{yy}\\ \gamma_{xy}\end{pmatrix}, \tag{3}$$

where E, G and ϑ are the Young's modulus, shear modulus and Poisson's ratio, respectively. In the continuation of this paper, we use expression (3) to derive governing equations for vibration and buckling load of MNPS.

3. Mathematical model of m-coupled nanoplates

Consider a set of m isotropic elastic nanoplates embedded in an elastic medium, as shown in Fig. 1. We assume that all nanoplates are made of a same material and with same dimensions such as uniform cross-section area A, thickness h, **length** a, **width** b, same elastic modulus E, Poisson's coefficient ϑ, shear modulus G and mass density ρ. In addition, we assume that the material of the elastic matrix, which is located between nanoplates, is described by a continuously distributed linear elastic springs, i.e. Winkler's elastic medium. The elastic medium is of stiffness $k_i, i = 1,2,3,\ldots,m$. In general, we may consider different types of medium between nanoplates, etc. viscoelastic medium with different viscoelastic models, elastic medium by Pasternak model and others. Each nanoplate is under the influence of biaxial compression loads N_x and N_y in x and y directions (see Fig. 1(b) and (c)). The transverse displacements of m-coupled nanoplates are denoted by $w_i(x,y,t)$, $(i = 1,2,3,\ldots,m)$. This study is limited to the case of the nonlocal Kirchhoff–Love plate theory and simply supported boundary conditions. In addition, we will consider two different chain systems. In the case of "Clamped-Chain" system, the first and the last nanoplate in the system are coupled with a fixed base by the Winkler elastic medium of stiffness of k_0 and k_m, respectively, as shown in Fig. 1b). In the case of "Free-Chain" system the stiffness's of Winkler elastic medium k_0 and k_m are vanishes (see Fig. 1c)), i.e. there

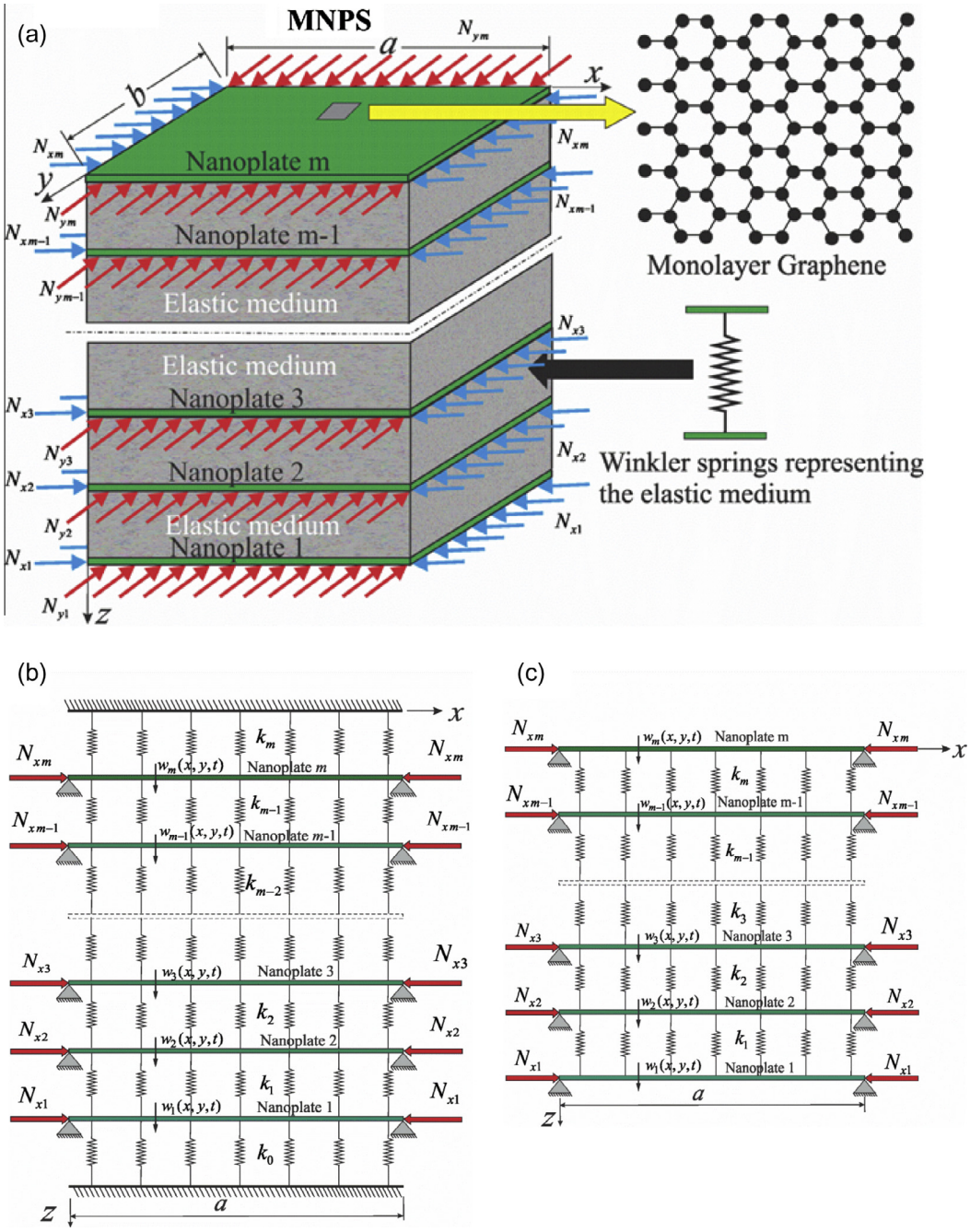

Fig. 1. Multi-nanoplate system: (a) schematic diagram of graphene sheets embedded in an elastic medium; (b) Clamped-Chain system; (c) Free-Chain system.

is no coupling with the fixed base. The x and y are the coordinates in the directions of width and length of nanoplates, while z is the coordinate in the direction of the thickness.

According to the Kirchhoff–Love plate theory, displacement components (u_{ix}, v_{iy}, w_{iz}) defined for an arbitrary point of the middle surface of ith nanoplate as

$$u_{ix} = -z\frac{\partial w_i}{\partial x}, v_{iy} = -z\frac{\partial w_i}{\partial y}, w_{iz} = w_i(x,y,t), \tag{4}$$

where u_{ix} and v_{iy} are in plane rotation displacements of nanoplates and w_{iz} is a transverse displacement. Based on the given displacement field and assuming small deformations, we can obtain non-zero strain–displacement relations as

$$\varepsilon_{xx} = -z\frac{\partial^2 w_i}{\partial x^2}, \ \varepsilon_{yy} = -z\frac{\partial^2 w_i}{\partial y^2}, \ \gamma_{xy} = -2z\frac{\partial^2 w_i}{\partial x \partial y}, \tag{5}$$

where ε_{xx} and ε_{yy} are normal strains, and γ_{xy} is a shear strain. Using the D'Alembert's principle, we get the equilibrium equations expressed through stress resultants terms in the following form

$$q + N_x\frac{\partial^2 w_i}{\partial x^2} + N_y\frac{\partial^2 w_i}{\partial y^2} + \frac{\partial Q_x}{\partial x} + \frac{\partial Q_y}{\partial y} = \rho h\frac{\partial^2 w_i}{\partial t^2}, \tag{6a}$$

$$\frac{\partial M_x}{\partial x} + \frac{\partial M_{xy}}{\partial y} = Q_x, \tag{6b}$$

$$\frac{\partial M_y}{\partial y} + \frac{\partial M_{xy}}{\partial x} = Q_y. \tag{6c}$$

Introducing expressions (6a) and (6b) into the first equilibrium Eq. (6a) leads to the governing equation of motion of ith nanoplate of the form

$$q + N_x\frac{\partial^2 w_i}{\partial x^2} + N_y\frac{\partial^2 w_i}{\partial y^2} + \frac{\partial^2 M_x}{\partial x^2} + \frac{\partial^2 M_y}{\partial y^2} + 2\frac{\partial^2 M_{xy}}{\partial x \partial y} = \rho h\frac{\partial^2 w_i}{\partial t^2}, \tag{7}$$

where M_x and M_y are bending moments and M_{xy} is a twisting moment

$$(M_x, M_y, M_{xy}) = \int_{-h/2}^{h/2} (\sigma_{xx}, \sigma_{yy}, \tau_{xy}) z dz. \tag{8}$$

External load from Winkler elastic medium defined as

$$q = F_{ki} - F_{ki-1} = k_i(w_{i+1} - w_i) - k_{i-1}(w_i - w_{i-1}). \tag{9}$$

By substituting Eq. (5) into Eq. (3) and then using expression (8) leads to

$$(1 - \mu\Delta)M_x = -D\left(\frac{\partial^2 w_i}{\partial x^2} + \vartheta\frac{\partial^2 w_i}{\partial y^2}\right), \tag{10a}$$

$$(1 - \mu\Delta)M_y = -D\left(\frac{\partial^2 w_i}{\partial y^2} + \vartheta\frac{\partial^2 w_i}{\partial x^2}\right), \tag{10b}$$

$$(1 - \mu\Delta)M_{xy} = -D(1 - \vartheta)\frac{\partial^2 w_i}{\partial x \partial y}, \tag{10c}$$

where $D = Eh^3/[12(1 - \vartheta^2)]$ is bending rigidity of a nanoplate. Finally, using Eqs. (7) and (10) we obtain partial differential equations of motion in terms of transversal displacements

$$\begin{aligned}
&\rho h\frac{\partial^2 w_i}{\partial t^2} + k_i(w_i - w_{i+1}) + k_{i-1}(w_i - w_{i-1}) \\
&+ D\left(\frac{\partial^4 w_i}{\partial x^4} + \frac{\partial^4 w_i}{\partial y^4} + 2\frac{\partial^2 w_i}{\partial x^2 \partial y^2}\right) - N_x\frac{\partial^2 w_i}{\partial x^2} - N_y\frac{\partial^2 w_i}{\partial y^2} \\
&= \mu\frac{\partial^2}{\partial x^2}\left(\rho h\frac{\partial^2 w_i}{\partial t^2} + k_i(w_i - w_{i+1}) + k_{i-1}(w_i - w_{i-1}) - N_x\frac{\partial^2 w_i}{\partial x^2} - N_y\frac{\partial^2 w_i}{\partial y^2}\right) \\
&\quad + \mu\frac{\partial^2}{\partial y^2}\left(\rho h\frac{\partial^2 w_i}{\partial t^2} + k_i(w_i - w_{i+1}) + k_{i-1}(w_i - w_{i-1}) - N_x\frac{\partial^2 w_i}{\partial x^2} - N_y\frac{\partial^2 w_i}{\partial y^2}\right),
\end{aligned} \tag{11}$$

for $i = 1,2,3\ldots,m$.

Assuming that the all-rectangular nanoplates in MNPS are having same simply supported boundary conditions at all four edges, we can write the following

$$w_i(x,0,t) = w_i(x,b,t) = 0, \quad w_i(0,y,t) = w_i(a,y,t) = 0, \quad i = 1,2,3,\ldots,m. \tag{12a}$$

$$M_{xi}(0,y,t) = M_{xi}(a,y,t) = 0, \quad M_{yi}(x,0,t) = M_{yi}(x,b,t) = 0. \tag{12b}$$

4. Analytical solutions

An analytical solution for system of simply supported nanoplates can be obtained by introducing Navier's solutions, as shown in many papers [42–45] and books [71,72]. In order to solve the equations of motion for proposed system of coupled nanoplates, we assumed the solution by the following expansions of generalized displacements $w_i(x,t)$

$$w_i(x,y,t) = \sum_{n=1}^{\infty} W_{irn} \sin\alpha_r x \sin\beta_n y e^{j\omega_{rn}t}, \quad i = 1,2,3,\ldots,m, \tag{13}$$

where $j = \sqrt{-1}$ $\alpha_r = \frac{r\pi}{a}; \beta_n = \frac{n\pi}{b} (r,n = 1,2,3,\ldots)$; W_{irn}, ω_{rn}(i = 1,2,3, …,m) are amplitudes and natural frequencies, respectively. Substituting expressions for the assumed solution (13) into the equation of motion (11), we obtain the system of m algebraic equations of the form

$$-v_{i-1rn}W_{i-1rn} + S_{irn}W_{irn} - v_{irn}W_{i+1rn} = 0, \ i = 1,2,3,\ldots,m, \tag{14}$$

where

$$\begin{aligned}
S_{irn} &= -\rho h\omega_{rn}^2\xi_{rn} + D\left(\alpha_r^2 + \beta_n^2\right)^2 + N_x\left(\alpha_r^2 + \delta\beta_n^2\right)\xi_{rn} \\
&\quad + v_{irn} + v_{i-1rn},
\end{aligned} \tag{15a}$$

$$v_{irn} = k_i\xi_{rn}, \tag{15b}$$

$$v_{i-1rn} = k_{i-1}\xi_{rn}, \tag{15c}$$

$$\xi_{rn} = \left(1 + \mu\alpha_r^2 + \mu\beta_n^2\right). \tag{15d}$$

in which $\delta = N_y/N_x$ define the relation between biaxial compression loads N_x and N_y.

Introducing dimensionless parameters

$$\Omega_{rn} = \omega_{rn}a^2\sqrt{\frac{\rho h}{D}}, \quad \widehat{N} = -N_x\frac{a^2}{D}, \quad R = \frac{a}{b}, \quad K_i = k_i\frac{a^4}{D},$$
$$\eta^2 = \frac{\mu}{a^2} = \frac{(e_0\tilde{a})^2}{a^2}, \tag{16}$$

where η is the nonlocal parameter in dimensionless form, μ is the nonlocal parameter and a is the length of a nanoplate (Fig. 1).

we can rewrite Eq. (15) as

$$\begin{aligned}
\widehat{S}_{irn} &= -\Omega_{rn}^2\hat{\xi}_{rn} + \left[(r\pi)^2 + R^2(n\pi)^2\right]^2 - \widehat{N}\left[(r\pi)^2 + \delta R^2(n\pi)^2\right]\hat{\xi}_{rn} \\
&\quad + \hat{v}_{irn} + \hat{v}_{i-1rn},
\end{aligned} \tag{17a}$$

$$\hat{v}_{irn} = K_i\hat{\xi}_{rn}, \tag{17b}$$

$$\hat{v}_{i-1rn} = K_{i-1}\hat{\xi}_{rn}, \tag{17c}$$

$$\hat{\xi}_{rn} = 1 + \eta^2(r\pi)^2 + \eta^2R^2(n\pi)^2, \tag{17d}$$

where $\widehat{S}_{irn} = S_{irn}\frac{a^4}{D}$ and $\hat{v}_{irn} = v_{irn}\frac{a^4}{D}$.

4.1. Clamped-Chain system

Let us first consider a system of coupled identical nanoplates embedded in the Winkler elastic medium named "Clamped-Chain" system, where the first and the last nanoplate in the system are elastically connected with the fixed base. Coupling conditions for this system are

$$K_0 \neq 0, K_m \neq 0 \text{ and } W_{0rn} = 0, W_{m+1rn} = 0. \tag{18}$$

Introducing expression (18) into Eq. (14) and assuming that stiffnesses of elastic layers between nanoplates are same, we obtain the system of algebraic Eq. (14) in the following form

$$\begin{bmatrix}
\widehat{S}_{rn} & -\hat{v}_{rn} & 0 & \ldots & 0 & 0 & 0 & \ldots & 0 & 0 & 0 \\
-\hat{v}_{rn} & \widehat{S}_{rn} & -\hat{v}_{rn} & \ldots & 0 & 0 & 0 & \ldots & 0 & 0 & 0 \\
\ldots & \ldots & \ldots & \ldots & \ldots & \ldots & \ldots & \ldots & \ldots & \ldots & \ldots \\
0 & 0 & 0 & \ldots & \widehat{S}_{rn} & -\hat{v}_{rn} & 0 & \ldots & 0 & 0 & 0 \\
0 & 0 & 0 & \ldots & -\hat{v}_{rn} & \widehat{S}_{rn} & -\hat{v}_{rn} & \ldots & 0 & 0 & 0 \\
0 & 0 & 0 & \ldots & 0 & -\hat{v}_{rn} & \widehat{S}_{rn} & \ldots & 0 & 0 & 0 \\
\ldots & \ldots & \ldots & \ldots & \ldots & \ldots & \ldots & \ldots & \ldots & \ldots & .. \\
0 & 0 & 0 & \ldots & 0 & 0 & 0 & \ldots & 0 & \widehat{S}_{rn} & -\hat{v}_{rn} \\
0 & 0 & 0 & \ldots & 0 & 0 & 0 & \ldots & 0 & -\hat{v}_{rn} & \widehat{S}_{rn}
\end{bmatrix}
\begin{Bmatrix}
W_{1rn} \\ W_{2rn} \\ W_{3rn} \\ \ldots \\ W_{i-1rn} \\ W_{irn} \\ W_{i+1rn} \\ \ldots \\ W_{m-2rn} \\ W_{m-1rn} \\ W_{mrn}
\end{Bmatrix} =
\begin{Bmatrix}
0 \\ 0 \\ 0 \\ \ldots \\ 0 \\ 0 \\ 0 \\ \ldots \\ 0 \\ 0 \\ 0
\end{Bmatrix} \tag{19}$$

where

$$\widehat{S}_{rn} = -\Omega_{rn}^2\hat{\xi}_{rn} + \left[(r\pi)^2 + R^2(n\pi)^2\right]^2 - \widehat{N}\left[(r\pi)^2 + \delta R^2(n\pi)^2\right]\hat{\xi}_{rn} + 2\hat{v}_{rn}, \tag{20a}$$

$$\hat{v}_{rn} = K\hat{\xi}_{rn}. \tag{20b}$$

The closed form solutions for dimensionless natural frequencies and buckling load are obtained by using the trigonometric method, as shown in papers [73–75]. In addition, it should be noted that the analytical solution for the homogenous system of algebraic Eq. (19) is possible only under the assumption that the system is made of a set of m identical nanoplates and identical coupling layers. Based on the methodology presented in [74], we assumed solution of $i - th$ algebraic equation in the form

$$W_{irn} = Ncos(i\varphi_{cc}) + Msin(i\varphi_{cc}), \ i = 1,2,3,\ldots,m. \tag{21}$$

By substituting assumed solution (21) into the ith algebraic equation of system (19), we get system of two algebraic equations, where the constants M and N are not simultaneously equal to zero

$$\begin{aligned}
&N\{-\hat{v}_{rn}cos[(i-1)\varphi_{cc}] + \widehat{S}_{rn}cos(i\varphi_{cc}) - \hat{v}_{rn}cos[(i+1)\varphi_{cc}]\} \\
&= 0, \quad i = 2,3,\ldots,m-1,
\end{aligned} \tag{22a}$$

$$M\{-\hat{v}_{rn}sin[(i-1)\varphi_{cc}]+\widehat{S}_{rn}sin(i\varphi_{cc})-\hat{v}_{rn}sin[(i+1)\varphi_{cc}]\} = 0, \quad i=2,3,\ldots,m-1, \tag{22b}$$

where after simplification we obtain

$$(\widehat{S}_{rn}-2\hat{v}_{rn}cos\varphi_{cc})N\ cos(i\varphi_{cc})=0, \tag{23a}$$

$$(\widehat{S}_{rn}-2\hat{v}_{rn}cos\varphi_{cc})M\ sin(i\varphi_{cc})=0, \tag{23b}$$

in which, $N\neq 0$ and $cos(i\varphi_{cc})\neq 0$ or $M\neq 0$ and $sin(i\varphi_{cc})\neq 0$ for the case when system has an oscillatory behavior, for $i=2,3,\ldots,m-1$. From expressions (23), we get the frequency and stability equation

$$\widehat{S}_{rn}=2\hat{v}_{rn}cos\varphi_{cc}, \tag{24}$$

where φ_{cc} is an unknown parameter, which is determined from the first and the last equation of the system of algebraic Eq. (19) i.e. from the boundary conditions of the chain system. Introducing assumed solutions from Eq. (21) i.e. $W_{1rn}=N\ cos\varphi_{cc}+M\ sin\varphi_{cc}$ and $W_{2rn}=N\ cos(2\varphi_{cc})+M\ sin(2\varphi_{cc})$ into the first equation and $W_{m-1rn}=N\ cos[(m-1)\varphi_{cc}]+M\ sin[(m-1)\varphi_{cc}]$ and $W_{m-1rn}=N\ cos(m\varphi_{cc})+M\ sin(m\varphi_{cc})$ into the last equation of the system (19), yields

$$N[\widehat{S}_{rn}cos\varphi_{cc}-\hat{v}_{rn}cos(2\varphi_{cc})]+M[\widehat{S}_{rn}sin\varphi_{cc}-\hat{v}_{rn}sin(2\varphi_{cc})]=0, \tag{25a}$$

$$N[\widehat{S}_{rn}cos(m\varphi_{cc})-\hat{v}_{rn}cos[(m-1)\varphi_{cc}]]+M[\widehat{S}_{rn}sin(m\varphi_{cc}) -\hat{v}_{rn}sin[(m-1)\varphi_{cc}]]=0. \tag{25b}$$

From the system of trigonometric Eqs. (25), we obtain the determinant where non-trivial solutions solution yields the unknown φ_{cc}

$$\begin{vmatrix} 1 & 0 \\ cos[(m+1)\varphi_{cc}] & sin[(m+1)\varphi_{cc}] \end{vmatrix}=0\Rightarrow sin[(m+1)\varphi_{cc}]=0, \tag{26}$$

in which $\varphi_{cc,s}$ has the following form

$$\varphi_{cc,s}=\frac{s\pi}{m+1}, s=1,2,\ldots,m. \tag{27}$$

Introducing Eq. (27) $\varphi_{cc,s}$and Eq. (20) into the Eq. (24), we get the frequency and stability equation as

$$-\Omega_{rn}^2\hat{\xi}_{rn}+[(r\pi)^2+R^2(n\pi)^2]^2-\widehat{N}_{rn}[(r\pi)^2+\delta R^2(n\pi)^2]\hat{\xi}_{rn} +2\hat{v}_{rn}(1-cos\varphi_{cc,s}) =0. \tag{28}$$

For the case when $\widehat{N}=0$, from Eq. (28) we obtain the natural frequency of elastic MNPS as

$$\Omega_{rncc,s}=\sqrt{\frac{[(r\pi)^2+R^2(n\pi)^2]^2+2K(1+\eta^2(r\pi)^2+\eta^2R^2(n\pi)^2)(1-cos\varphi_{cc,s})}{1+\eta^2(r\pi)^2+\eta^2R^2(n\pi)^2}}, \quad s=1,2,\ldots,m, \tag{29}$$

When the bi-axial load applied to each nanoplate in MNPS reaches a certain critical value, MNPS becomes unstable and we can consider that system begins to buckle. Introducing $\Omega_{rn}=0$ into Eq. (28) gives

$$\widehat{N}_{rncc,s}=\frac{[(r\pi)^2+R^2(n\pi)^2]^2+2K(1+\eta^2(r\pi)^2+\eta^2R^2(n\pi)^2)(1-cos\varphi_{cc,s})}{[(r\pi)^2+\delta R^2(n\pi)^2](1+\eta^2(r\pi)^2+\eta^2R^2(n\pi)^2)}, \quad s=1,2,\ldots,m, \tag{30}$$

4.2. Free-Chain system

Here, we consider the system where the first and the last nanoplate are without coupling with the fixed base where coupling conditions are $K_0=0$ and $K_m=0$. Also, it is assumed that the system is consist of identical nanoplates coupled by the same Winkler elastic layers. The system of algebraic Eq. (14) in the case of "Free-Chain" system is

$$\begin{bmatrix} \widehat{S}_{rn}-\hat{v}_{rn} & -\hat{v}_{rn} & 0 & \ldots & 0 & 0 & 0 & \ldots & 0 & 0 & 0 \\ -\hat{v}_{rn} & \widehat{S}_{rn} & -\hat{v}_{rn} & \ldots & 0 & 0 & 0 & \ldots & 0 & 0 & 0 \\ \ldots & \ldots & \ldots & \ldots & \ldots & \ldots & \ldots & \ldots & \ldots & \ldots & \ldots \\ 0 & 0 & 0 & \ldots & \widehat{S}_{rn} & -\hat{v}_{rn} & 0 & \ldots & 0 & 0 & 0 \\ 0 & 0 & 0 & \ldots & -\hat{v}_{rn} & \widehat{S}_{rn} & -\hat{v}_{rn} & \ldots & 0 & 0 & 0 \\ 0 & 0 & 0 & \ldots & 0 & -\hat{v}_{rn} & \widehat{S}_{rn} & \ldots & 0 & 0 & 0 \\ \ldots & \ldots & \ldots & \ldots & \ldots & \ldots & \ldots & \ldots & \ldots & \ldots & .. \\ 0 & 0 & 0 & \ldots & 0 & 0 & 0 & \ldots & 0 & \widehat{S}_{rn} & -\hat{v}_{rn} \\ 0 & 0 & 0 & \ldots & 0 & 0 & 0 & \ldots & 0 & -\hat{v}_{rn} & \widehat{S}_{rn}-\hat{v}_{rn} \end{bmatrix} \begin{Bmatrix} W_{1rn} \\ W_{2rn} \\ W_{3rn} \\ \ldots \\ W_{i-1rn} \\ W_{irn} \\ W_{i+1rn} \\ \ldots \\ W_{m-2rn} \\ W_{m-1rn} \\ W_{mrn} \end{Bmatrix} = \begin{Bmatrix} 0 \\ 0 \\ 0 \\ \ldots \\ 0 \\ 0 \\ 0 \\ \ldots \\ 0 \\ 0 \\ 0 \end{Bmatrix} \tag{31}$$

where expressions $\widehat{S}_{rn}$ and $\hat{v}_{rn}$ are defined in Eq. (20).

Substituting Eq. (21) into ith algebraic equation of system (31), we get the frequency and stability equation as for the previous case

$$\widehat{S}_{rn}=2\hat{v}_{rn}cos\varphi_{fc}, \tag{32}$$

where φ_{fc} is an unknown parameter, which is determined from the first and the last equation of the system of algebraic Eq. (31) i.e. boundary conditions of the "Free-Chain" system. Introducing assumed solutions for the first and the second amplitude,$W_{1rn}=N\ cos\varphi_{fc}+M\ sin\varphi_{fc}$ and $W_{2rn}=N\ cos(2\varphi_{fc})+M\ sin(2\varphi_{fc})$, into the first equation and $W_{m-1n}=N\ cos[(m-1)\varphi_{fc}]+M\ sin[(m-1)\varphi_{fc}]$ and $W_{m-1n}=N\ cos(m\varphi_{fc})+M\ sin(m\varphi_{fc})$ into the last equation of system (31), after some transformations we get

$$N[(\widehat{S}_{rn}-\hat{v}_{rn})cos\varphi_{fc}-\hat{v}_{rn}cos(2\varphi_{fc})]+M[(\widehat{S}_{rn}-\hat{v}_{rn})sin\varphi_{fc} -\hat{v}_{rn}sin(2\varphi_{fc})]=0, \tag{33a}$$

$$N[(\widehat{S}_{rn}-\hat{v}_{rn})cos(m\varphi_{fc})-\hat{v}_{rn}cos[(m-1)\varphi_{fc}]] +M[(\widehat{S}_{rn}-\hat{v}_{rn})sin(m\varphi_{fc})-\hat{v}_{rn}sin[(m-1)\varphi_{fc}]]=0. \tag{33b}$$

Starting from the system of algebraic Eqs. (33) leads to the trigonometric equations of the form

$$\begin{vmatrix} 1-cos\varphi_{fc} & -sin\varphi_{fc} \\ cos[(m+1)\varphi_{cc}]-cos(m\varphi_{fc}) & sin[(m+1)\varphi_{cc}]-sin(m\varphi_{fc}) \end{vmatrix}=0\Rightarrow sin(m\varphi_{fc})=0, \tag{34}$$

where unknown $\varphi_{fc,s}$ is equal to

$$\varphi_{fc,s}=\frac{s\pi}{m},\ s=0,1,\ldots,m-1. \tag{35}$$

Introducing expression for parameter $\varphi_{fc,s}$ and Eq. (20) into Eq. (32), we obtain the frequency and stability equation in the following form

$$-\Omega_{rn}^2\hat{\xi}_{rn}+[(r\pi)^2+R^2(n\pi)^2]^2-\widehat{N}_{rn}[(r\pi)^2+\delta R^2(n\pi)^2]\hat{\xi}_{rn} +2\hat{v}rn\left(1-cos\varphi_{fc,s}\right) =0. \tag{36}$$

For the case when $\widehat{N}=0$, from Eq. (36) we obtain the natural frequency of elastic MNPS as

$$\Omega_{rnfc,s}=\sqrt{\frac{[(r\pi)^2+R^2(n\pi)^2]^2+2K(1+\eta^2(r\pi)^2+\eta^2R^2(n\pi)^2)(1-cos\varphi_{fc,s})}{1+\eta^2(r\pi)^2+\eta^2R^2(n\pi)^2}}, \quad s=0,1,\ldots,m-1, \tag{37}$$

Same as in the previous case, when the bi-axial load applied to each nanoplate in MNPS reaches a certain critical value, MNPS becomes unstable and we can consider that system begins to buckle. Introducing $\Omega_{rn}=0$ into Eq. (36) gives

$$\widehat{N}_{rnfc,s}=\frac{\left[(r\pi)^2+R^2(n\pi)^2\right]^2+2K(1+\eta^2(r\pi)^2+\eta^2R^2(n\pi)^2)(1-cos\varphi_{fc,s})}{[(r\pi)^2+\delta R^2(n\pi)^2](1+\eta^2(r\pi)^2+\eta^2R^2(n\pi)^2)},\quad s=0,1,\ldots,m-1, \tag{38}$$

4.3. Asymptotic analysis and analytical validation

When the number of nanoplates in the elastic MNPS, increase to the infinity, i.e. entering $m\to\infty$ into Eqs. (29) and (37) or Eqs. (30) and (38), we obtain critical natural frequency and **critical buckling load** such as

$$\Omega_{\substack{rn\\m\to\infty}}=\sqrt{\frac{\left[(r\pi)^2+R^2(n\pi)^2\right]^2}{1+\eta^2(r\pi)^2+\eta^2R^2(n\pi)^2}}, \tag{39a}$$

$$\widehat{N}_{\substack{rn\\m\to\infty}}=\frac{\left[(r\pi)^2+R^2(n\pi)^2\right]^2}{[(r\pi)^2+\delta R^2(n\pi)^2](1+\eta^2(r\pi)^2+\eta^2R^2(n\pi)^2)},\quad (r,n=1,2,\ldots). \tag{39b}$$

Finally, we can conclude that the critical natural frequency and **critical buckling load** represented by the expressions (39) are the natural frequency and **critical buckling load** of the system when the numbers of nanoplates are increased to the infinity. By the term critical, we are not always meaning the first mode frequency and buckling. It is observed that these critical values are independent of the chain boundary conditions and are same in both cases, "Clamped-Chain" and "Free-Chain" system.

Further, we validate our model and method analytically by considering the special case of MNPS composed of only two nanoplates coupled in "Free-Chain" system. It should be noted that in the literature we found exact solutions for natural frequencies and **critical buckling load** only for cases where maximum two coupled nanoplates are considered e.g. see Murmu and Adhikari [66,69]. For systems with three and more nanoplates, in the literature we found only numerical solutions for natural frequencies and **critical buckling load**. The obtained analytical expressions for the dimensionless natural frequency (37) and buckling load (38) are reduced to $s=0,1$ and $m=2$ in order to coincide with the expression for two coupled nanoplates proposed by Murmu and Adhikari [66,69]. Introducing $s=0$ and $m=2$ into Eqs. (37) and (38) yields the expressions

$$\Omega_{rnfc,0}=\sqrt{\frac{\left[(r\pi)^2+R^2(n\pi)^2\right]^2}{1+\eta^2(r\pi)^2+\eta^2R^2(n\pi)^2}}, \tag{40a}$$

$$\widehat{N}_{rnfc,0}=\frac{\left[(r\pi)^2+R^2(n\pi)^2\right]^2}{[(r\pi)^2+\delta R^2(n\pi)^2](1+\eta^2(r\pi)^2+\eta^2R^2(n\pi)^2)},\quad (r,n=1,2,\ldots), \tag{40b}$$

in which $\Omega_{rnfc,0}$ and $\widehat{N}_{rnfc,0}$ represents a synchronous modes of vibration and stability. For the second case or asynchronous modes of vibration and stability, we introduced $s=1$ and $m=2$ into Eqs. (37) and (38) where we obtained

$$\Omega_{rnfc,1}=\sqrt{\frac{\left[(r\pi)^2+R^2(n\pi)^2\right]^2+2K(1+\eta^2(r\pi)^2+\eta^2R^2(n\pi)^2)}{1+\eta^2(r\pi)^2+\eta^2R^2(n\pi)^2}}, \tag{41a}$$

$$\widehat{N}_{rnfc,1}=\frac{\left[(r\pi)^2+R^2(n\pi)^2\right]^2+2K(1+\eta^2(r\pi)^2+\eta^2R^2(n\pi)^2)}{[(r\pi)^2+\delta R^2(n\pi)^2](1+\eta^2(r\pi)^2+\eta^2R^2(n\pi)^2)},\quad (r,n=1,2,\ldots). \tag{41b}$$

Finally, it can be ascertained that obtained theoretical model represents a generalization of the vibration and stability problem for systems with multiple coupled nanoplates embedded in elastic medium. This model can be extended to consider the systems with nanoplates embedded in different type of mediums.

5. Results and discussions

Various materials nanoplate structures can be modeled via nonlocal elasticity model of MNPS. Theoretical analysis of mechanical behavior of such systems can be crucial for their application in nano devices. As reported in [11] buckling of golden nanoplates embedded in a polymer matrix is imposed by a surrounding medium. Vibration properties of systems with nanoplates dispersed in polymer matrix may be also important for their application in nanosensors and nanocomposites [11,15,19,26–30]. For an illustration, we consider MNPS as a system composed of multiple graphene sheets embedded in a polymer matrix. The following

Table 1
Comparison of analytical and numerical solutions for natural frequencies of elastically coupled MNPS.

Number of nanoplates	"Free-Chain" System			"Clamped-Chain" System	
		N.S.[a] of Eq. (31) ($\widehat{N}_m=0$)	A.S.[b] Eq. (37)	N.S.[a] of Eq. (19) ($\widehat{N}_m=0$)	A.S.[b] Eq. (29)
The natural frequencies of coupled MNPS					
$m=2$	1	8.102641359754337	8.10264135975433	12.870617584436328	12.870617584436328
	2	16.298858763876737	16.29885876387674	19.122050020978442	19.122050020978440
$m=5$	1	8.102641359754331	8.102641359754337	9.614973543796884	9.614973543796877
	2	10.190652487932876	10.190652487932857	12.870617584436213	12.870617584436328
	3	14.277583763711931	14.277583763711986	16.298858763876922	16.298858763876740
	4	18.095750768614074	18.095750768613915	19.122050020977852	19.122050020978440
	5	20.675013806036212	20.675013806036286	20.948935003042514	20.948935003042262
$m=10$	1	8.102641359756117	8.102641359754337	8.588026681485388	8.588026681485225
	2	8.685706289377503	8.685706289402773	9.869249740408922	9.869249740409114
	3	10.190652487940827	10.190652487932857	11.605199275155108	11.605199275141490
	4	12.169459583146475	12.169459583165843	13.511839045938950	13.511839045978320
	5	14.277583763760147	14.277583763711986	15.400968455233263	15.400968454942843
	6	16.298858763828850	16.298858763876740	17.149803632265010	17.149803633262350
	7	18.095750768947923	18.095750768613915	18.674469194094154	18.674469192059487
	8	19.575746408604815	19.575746408842146	19.915444852405102	19.915444855535080
	9	20.675013806069206	20.675013806036286	20.830350539684872	20.830350538842062
	10	21.350974222653280	21.350974222827220	21.390450946077390	21.390450947273200

[a] N.S. – Numerical Solutions.
[b] A.S. – Analytical Solutions.

Table 2
Comparison of analytical and numerical solutions for **critical buckling load** of elastically coupled MNPS.

Number of nanoplates	"Free-Chain" System			"Clamped-Chain" System	
		N.S.[c] of Eq. (31) ($\Omega_{rn}=0$)	A.S.[d] Eq. (38)	N.S.[c] of Eq. (19) ($\Omega_{rn}=0$)	A. S.[d] Eq. (30)
The **critical buckling load** *buckling load of coupled MNPS,*					
$m=2$	1	4.434679401304418	4.434679401304419	11.189424977460272	11.189424977460272
	2	17.944170553616118	17.94417055361612	24.698916129771966	24.698916129771973
$m=5$	1	4.4346794013044395	4.434679401304419	6.244608023513074	6.244608023513079
	2	7.014762626037857	7.014762626037962	11.189424977460298	11.189424977460272
	3	13.769508202194016	13.769508202193814	17.9441705536164	17.94417055361612
	4	22.118832905038456	22.118832905038428	24.698916129771334	24.698916129771973
	5	28.87357848119441	28.873578481194283	29.64373308371962	29.64373308371917
$m=10$	1	4.43467940130375	4.434679401304419	4.981908715865823	4.981908715865823
	2	5.095880961381969	5.095880961378354	6.579263394981978	6.579263394982316
	3	7.01476262603017	7.014762626037962	9.097335262368473	9.097335262385945
	4	10.00349088834649	10.003490888311653	12.332125110984935	12.332125110929688
	5	13.769508202105083	13.769508202193814	16.02156950497541	16.021569505120507
	6	17.94417055361673	17.94417055361612	19.86677160331807	19.866771602111736
	7	22.11883290508726	22.118832905038428	23.55621599538792	23.556215996302555
	8	25.88485021879722	25.88485021892059	26.791005847718235	26.7910058448463
	9	28.873578481444355	28.873578481194283	29.309077707986063	29.309077712249927
	10	30.7924601454757	30.792460145853894	30.906432392673373	30.906432391366423

[c] N.S. – Numerical Solutions.
[d] A.S. – Analytical Solutions.

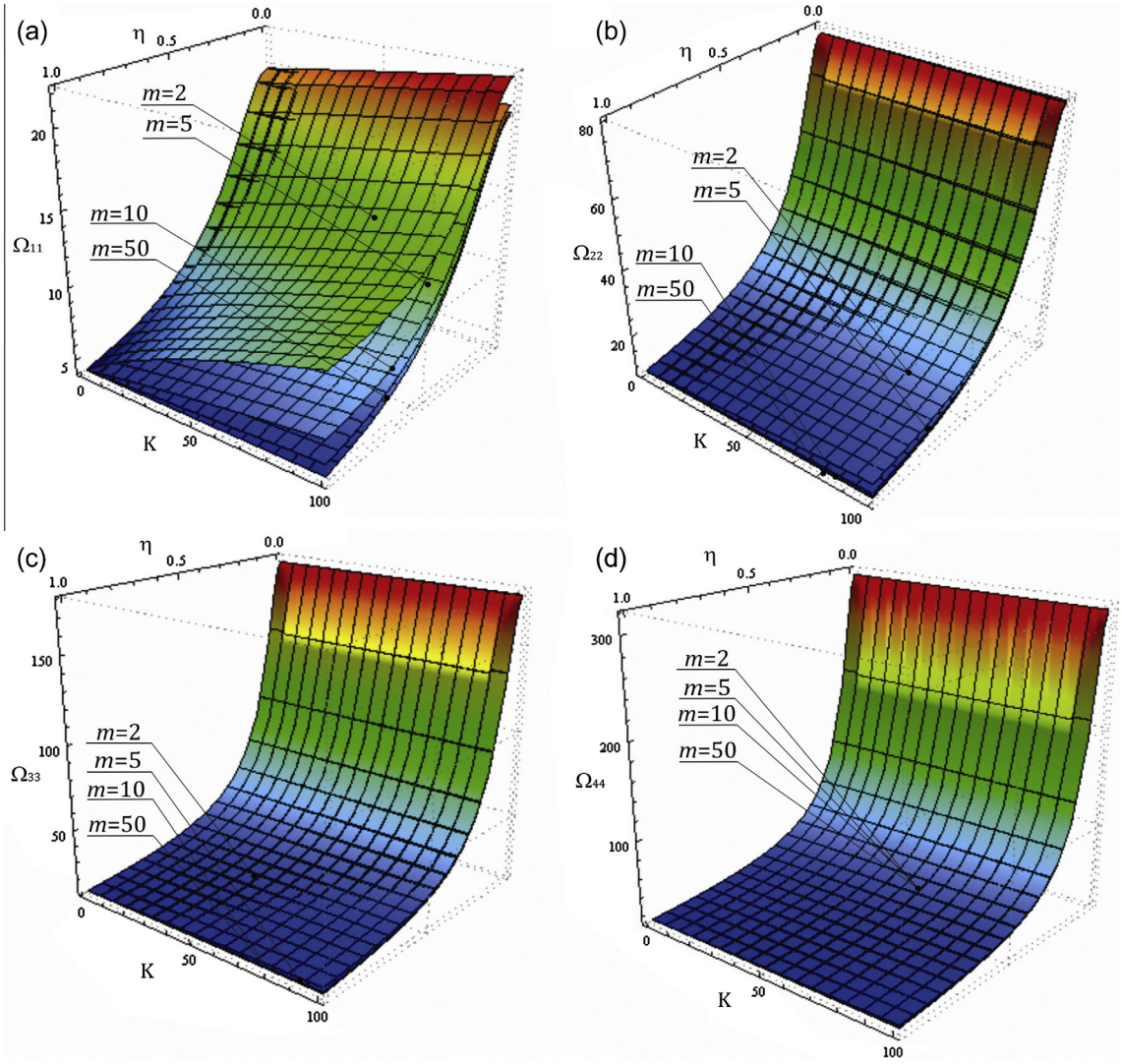

Fig. 2. The influence of the stiffness of Winkler elastic medium and nonlocal parameter on the natural frequencies for the "Clamped-Chain" system and different number of nanoplates, (a) mode $r=1$ and $n=1$, (b) mode $r=2$ and $n=2$, c) mode $r=3$ and $n=3$, d) mode $r=4$ and $n=4$.

material properties of graphene sheets similar to those in [66] are assumed: Young's modulus $E = 1.06$ TPa, Poisson's ratio $\vartheta = 0.25$, density $\rho = 2250$ kg/m^3 and thickness $h = 0.34$ nm. Natural frequencies and **critical buckling load** for MNPS are computed according to Eqs. (29), (30), (37) and (38).

5.1. Comparison of analytical and numerical solutions

To justify the proposed trigonometric solution for natural frequencies and buckling load we compared analytical solutions of homogenous system of algebraic equations against the numerical solution of the same system of equations. We must note that in follow all plotted quantities are dimensionless. For the comparison we considered the case when moder = 1, $n = 1$ and with aspect ratio $R = 1$, axial force ratio $\delta = 0.5$, nonlocal parameter $\eta = 0.5$ and stiffness coefficient $K = 100$. As shown in Table 1 for natural frequencies and in Table 2 for buckling load, compared values are in excellent agreement for both cases. It can be noticed that the lowest natural frequency of MNPS does not depend of the number of nanoplates in the Free-Chain system ($s = 0$). In the case of Clamped-Chain system, the natural frequency decreases towards the lowest natural frequency of the system when increasing the number of nanoplates in MNPS. The same can be observed for the lowest value of **critical buckling load** for Free-Chain and Clamped-Chain systems. All this alludes that applied trigonometric method for finding the exact analytical solution is reliable method for analysis of MNPS.

5.2. Effects of small-scale and coupling springs on vibration and buckling of MNPS

Following plots are performed for the next values: aspect ratio $R = 1$, axial force ratio $\delta = 0.5$, nonlocal parameter in the range $\eta = 0$–1, stiffness coefficient in the range $K = 0$–100 and $s = 1$. Fig. 2 illustrate changes in natural frequencies $\Omega_{rn,s}$ of MNPS for "Clamped-Chain" system due to changes in nonlocal parameter and stiffness of the elastic medium for different number of nanoplates in the system. The presented plots are for four different modes: $r = 1$, $n = 1$; $r = 2$, $n = 2$; $r = 3$, $n = 3$ and $r = 4$, $n = 4$. It can be observe that in lower modes increase of nonlocal parameter

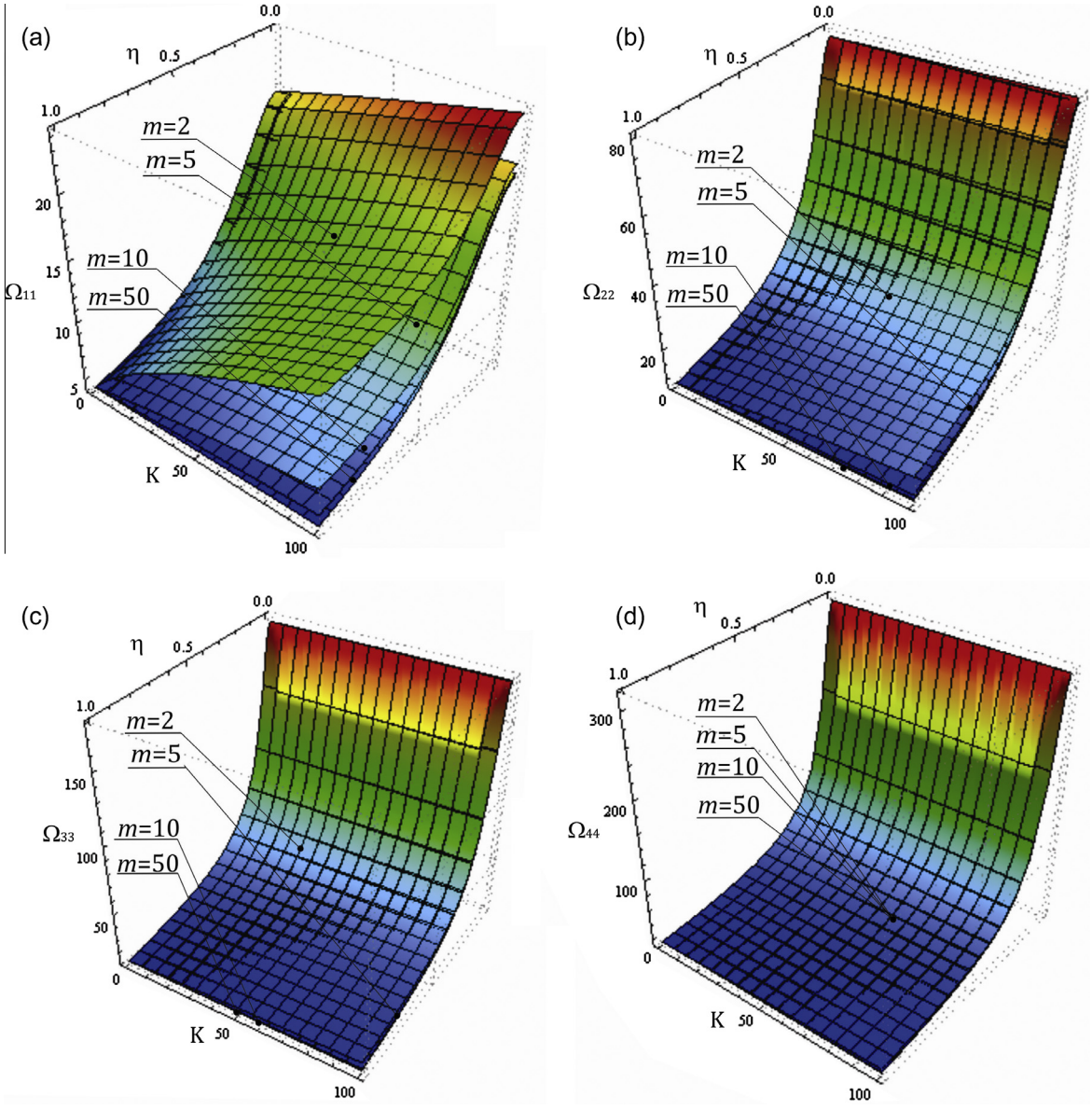

Fig. 3. The influence of the stiffness of Winkler elastic medium and nonlocal parameter on the natural frequencies for the "Free-Chain" system and different number of nanoplates, (a) mode $r = 1$ and $n = 1$, (b) mode $r = 2$ and $n = 2$, (c) mode $r = 3$ and $n = 3$, (d) mode $r = 4$ and $n = 4$.

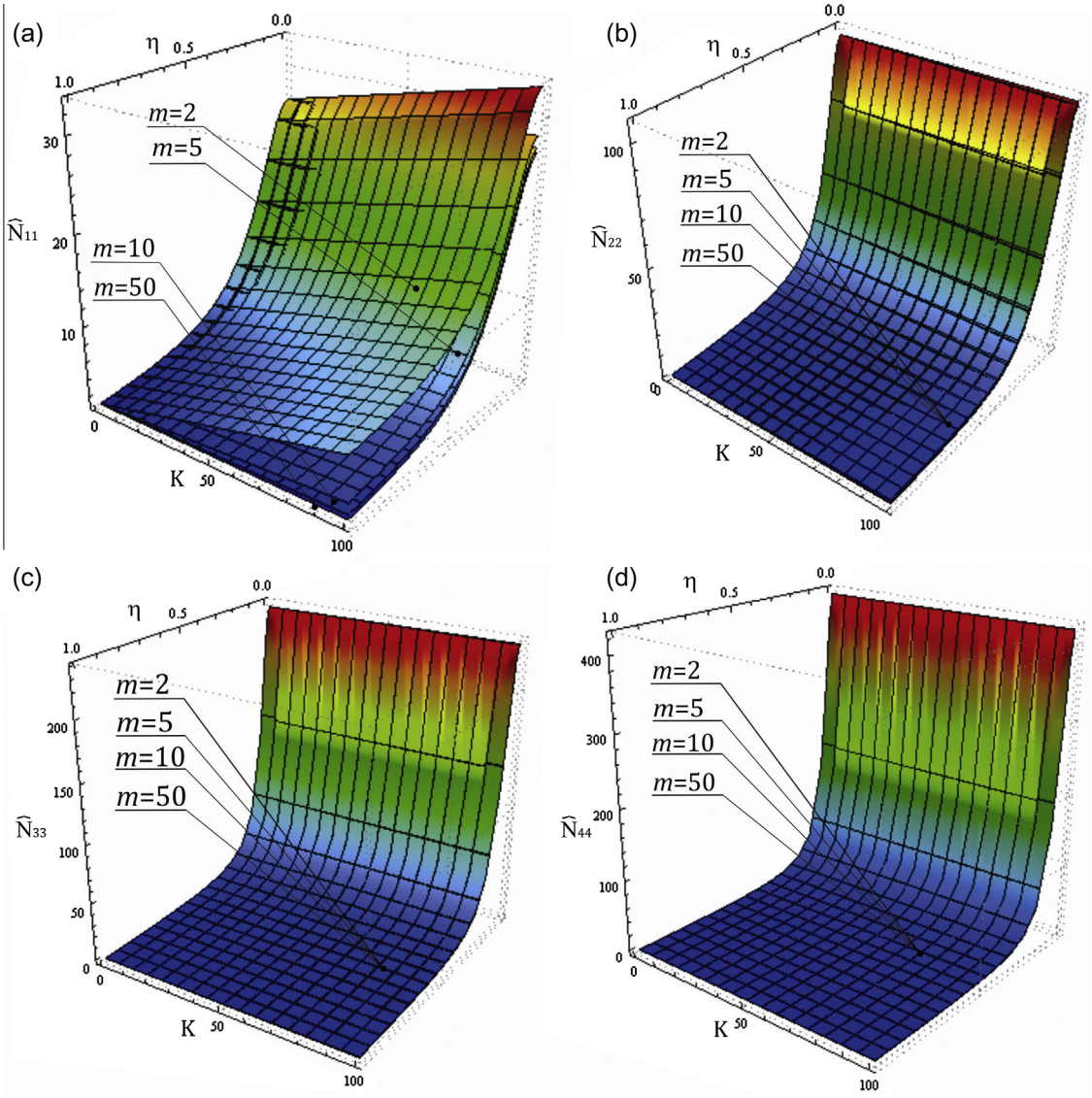

Fig. 4. The influence of the stiffness of Winkler elastic medium and nonlocal parameter on the **critical buckling load** for the "Clamped-Chain" system and different number of nanoplates, (a) mode $r = 1$ and $n = 1$, (b) mode $r = 2$ and $n = 2$, (c) mode $r = 3$ and $n = 3$, (d) mode $r = 4$ and $n = 4$.

causes a significant decrease of natural frequency while the increase of dimensionless stiffness coefficient causes a slight increase. When nonlocal parameter is equal to zero, natural frequencies are same as in case when using classical continuum theories, which, as obvious, over determine its values. The observation of increasing nonlocal parameter causing a significant decrease of natural frequency is in-line to that explained in Ref. [76] for a single nanoplate.

The consequence of increase of numbers of nanoplates in the system is that value of natural frequency is approaching towards certain constant value, which is in line with the asymptotic analysis of MNPS where for the increase of number of nanoplates in the system to infinity its value tends to the value of the lowest natural frequency of the system. In addition, it can be noticed that in higher modes, influence of nonlocal parameter is much more pronounced and we have significant decrease of natural frequencies for increase of the parameter. Opposite to this, change of elastic medium stiffness does not change natural frequencies considerably in lower modes and especially in higher modes. Effect of increase of nanoplates in MNPS is also less noticeable in higher modes than the lower one.

Fig. 3 illustrates effects of changes in nonlocal parameter, stiffness coefficient and number of nanoplates on natural frequencies of "Free-Chain" MNPS. The presented plots are for same modes as in the previous case. It can be noted that for lower modes natural frequencies are significantly decreases for increase of nonlocal parameter and slightly increase for increase of the stiffness coefficient. For this system, same as in Table 1 and Fig. 2, by increasing the number of nanoplates in the system we have decrease of natural frequencies, which is less pronounced in higher modes. Here, we can also notice a strong influence of nonlocal parameter on natural frequencies in higher modes while the influence of elastic medium stiffness becomes negligible.

The effect of dimensionless nonlocal parameter and stiffness coefficient of the layer on values of **critical buckling load** are shown in Fig. 4 for "Clamped-Chain" and in Fig. 5 for the "Free-Chain" MNPS. Effect of change of number of nanoplates in MNPS is also demonstrated. Similar to vibration analysis, following four modes are observed: $r = 1$, $n = 1$; $r = 2$, $n = 2$; $r = 3$, $n = 3$ and $r = 4$, $n = 4$. Obviously, buckling load is significantly influenced by the dimensionless nonlocal parameter i.e. increase of nonlocal parameter decrease value of **critical buckling load**. This effect is more

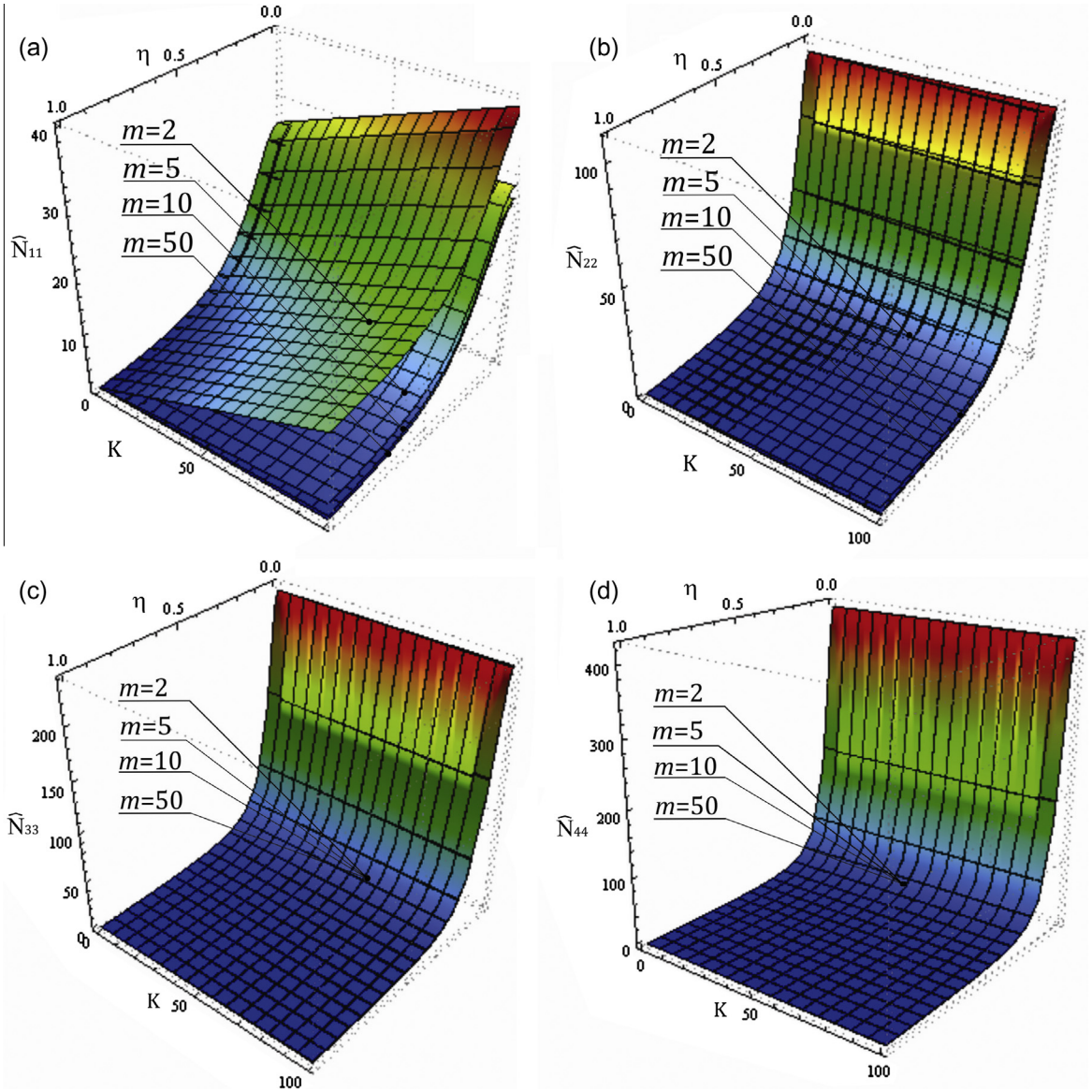

Fig. 5. The influence of the stiffness of Winkler elastic medium and nonlocal parameter on the **critical buckling load** buckling load for the "Free-Chain" system and different number of nanoplates, (a) mode $r = 1$ and $n = 1$, (b) mode $r = 2$ and $n = 2$, (c) mode $r = 3$ and $n = 3$, (d) mode $r = 4$ and $n = 4$.

pronounced in higher modes. The changes of stiffness coefficient slightly change the buckling load i.e. for the increase of stiffness of the medium in range 0–100 we have slight increase of buckling load. This increase is more pronounced in case of "Free-Chain" MNPS (Fig. 5) and for lower modes than for the "Clamped-Chain" MNPS (Fig. 4) and higher modes.

From Fig. 6(a) and (b) we can observe the influence of an increase of aspect ratio on natural frequencies and critical buckling load for different number of nanoplates in MNPS and both "Clamped-Chain" and "Free-Chain" system. In both figures, curves are plotted for the same values of parameters as in Tables 1 and 2. It is obvious that there is a significant difference between "Clamped-Chain" and "Free-Chain" systems when MNPS is composed of a small number of nanoplates. It can be noticed that the natural frequency and critical buckling load plotted for $s = 0$ in the case of "Free-Chain" system represents a fundamental natural frequency and critical buckling load which are independent of a number of nanoplates in MNPS. The previous conclusion is in line with the results presented in Tables 1 and 2 for the "Free-Chain" system. In the case of "Clamped-Chain" system the lowest natural frequency and critical buckling load are plotted for $s = 1$. It can be observed that an increase of a number of nanoplates in MNPS causes a decrease of natural frequencies and critical buckling loads towards the value of the lowest natural frequency and the lowest critical buckling load of the "Clamped-Chain" system i.e. these two values tends to the fundamental natural frequency and critical buckling load of the "Free-Chain" systems. This effect is also proved through the asymptotic analysis (Eq. (39)). The effect of an increase of the aspect ratio (R) reflects in an increase of natural frequencies of MNPS. This is in line with other results in the literature where an increase of any dimension of a structure leads to a decrease of the influence of small-scale parameter. In addition, from Fig. 6(b) it can be noticed that in the case of "Clamped-Chain" system for lower numbers of nanoplates in MNPS value of critical buckling load decreases for an increase of the aspect ratio. Hence, for higher numbers of nanoplates in MNPS value of critical buckling load slightly increases for an increase of the aspect ratio.

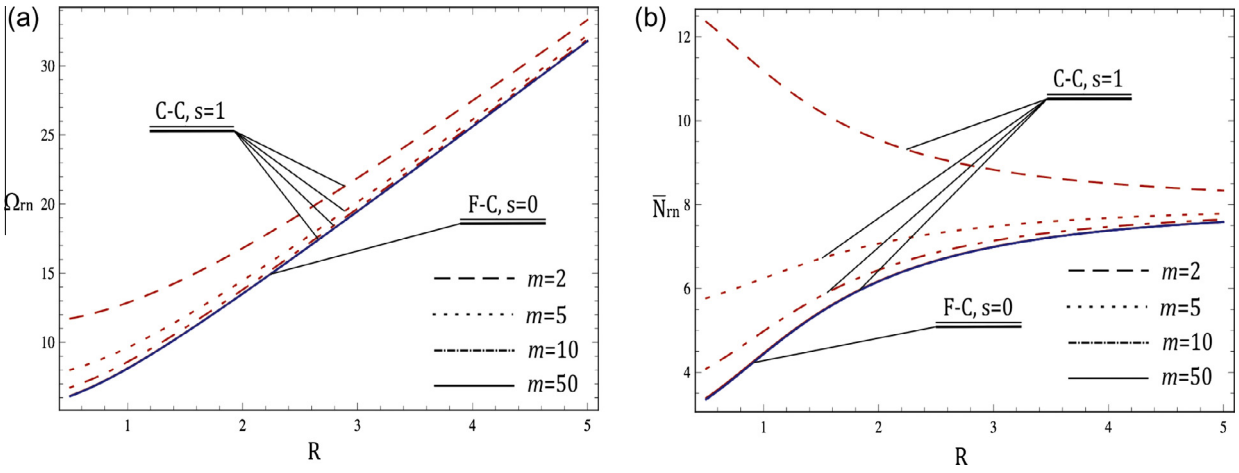

Fig. 6. The influence of the aspect ratio (R), (a) natural frequencies and (b) critical buckling load for the different number of nanoplates in the first mode.

6. Conclusion

Vibration and buckling study of a multi-nanoplate system embedded in the Winkler elastic medium is carried out using nonlocal elasticity theory. Exact analytical solutions of dimensionless natural frequencies and **critical buckling load** were derived for a different number of simply supported nanoplates in MNPS by using Navier's and trigonometric method. For the case of two coupled nanoplates, obtained results are validated with results available in the literature. In order to ensure the reliability of trigonometric method, analytical results for natural frequencies and buckling load obtained by solving the system of homogenous algebraic equations are compared with numerical solutions of the same system of equations for both chain conditions. Novel analytical expressions for critical values of the natural frequencies and **critical buckling load** are obtained by asymptotic analysis for the case when the number of nanoplates in MNPS tends to infinity. In addition, the effects of nonlocal parameter and stiffness of the Winkler elastic medium on natural frequencies and buckling load of MNPS in different modes are explored. Both the natural frequency and the **critical buckling load** are highly influenced by the small-scale effects, while the effect of the Winkler elastic medium decrease at higher modes. Regarding the effects of the number of nanoplates in MNPS, it was noticed that this effect has smaller influence on the natural frequencies and the **critical buckling load** at higher modes. Furthermore, it is found that the effect of change of nanoplate aspect ratio is more evident on natural frequencies than on the **critical buckling load**. Theoretical study performed here may be useful for practical design of nano-devices such as nanoresonators and for future investigations on other multiple-nanostructure systems embedded in different types of medium.

Acknowledgments

This research was supported by the research grant of the Serbian Ministry of Science and Environment Protection under the number of OI 174001.

References

[1] Geim AK, Novoselov KS. The rise of graphene. Nat Mater 2007;6(3):183–91.
[2] Meyer JC, Geim AK, Katsnelson MI, Novoselov KS, Booth TJ, Roth S. The structure of suspended graphene sheets. Nature 2007;446(7131):60–3.
[3] Liu M, Yin X, Ulin-Avila E, Geng B, Zentgraf T, Ju L, et al. A graphene-based broadband optical modulator. Nature 2011;4749(734):64–7.
[4] Ramanathan T, Abdala AA, Stankovich S, Dikin DA, Herrera-Alonso M, Piner RD, et al. Functionalized graphene sheets for polymer nanocomposites. Nat Nanotechnol 2008;3(6):327–31.
[5] Bunch JS, Van Der Zande AM, Verbridge SS, Frank IW, Tanenbaum DM, Parpia JM, et al. Electromechanical resonators from graphene sheets. Science 2007;315(5811):490–3.
[6] Stankovich S, Dikin DA, Dommett GH, Kohlhaas KM, Zimney EJ, Stach EA, et al. Graphene-based composite materials. Nature 2006;442(7100):282–6.
[7] Liu M, Yin X, Ulin-Avila E, Geng B, Zentgraf T, Ju L, et al. A graphene-based broadband optical modulator. Nature 2011;474(7349):64–7.
[8] Hao F, Fang D, Xu Z. Mechanical and thermal transport properties of graphene with defects. Appl Phys Lett 2011;99(4). 041901-041901.
[9] Xie J, Lee JY, Wang DI. Synthesis of single-crystalline gold nanoplates in aqueous solutions through biomineralization by serum albumin protein. J Phys Chem C 2007;111(28):10226–32.
[10] Fan X, Guo ZR, Hong JM, Zhang Y, Zhang JN, Gu N. Size-controlled growth of colloidal gold nanoplates and their high-purity acquisition. Nanotechnology 2010;21(10):105602.
[11] Porel S, Singh S, Radhakrishnan TP. Polygonal gold nanoplates in a polymer matrix. Chem Commun 2005(18):2387–9.
[12] Huang Z, Jiang X, Guo D, Gu N. Controllable synthesis and biomedical applications of silver nanomaterials. J Nanosci Nanotechnol 2011;11(11):9395–408.
[13] Liu Z, Zhou H, Lim YS, Song JH, Piao L, Kim SH. Synthesis of silver nanoplates by two-dimensional oriented attachment. Langmuir 2012;28(25):9244–9.
[14] Li N, Zhang Q, Quinlivan S, Goebl J, Gan Y, Yin Y. H_2O_2-aided seed-mediated synthesis of silver nanoplates with improved yield and efficiency. ChemPhysChem 2012;13(10):2526–30.
[15] Gao C, Lu Z, Liu Y, Zhang Q, Chi M, Cheng Q, et al. Highly stable silver nanoplates for surface plasmon resonance biosensing. Angew Chem Int Ed 2012;51(23):5629–33.
[16] Pacile D, Meyer JC, Girit CO, Zettl A. The two-dimensional phase of boron nitride: few-atomic-layer sheets and suspended membranes. Appl Phys Lett 2008;92(13). 133107-133107.
[17] Golberg D, Bando Y, Huang Y, Terao T, Mitome M, Tang C, et al. Boron nitride nanotubes and nanosheets. Acs Nano 2010;4(6):2979–93.
[18] Song L, Ci L, Lu H, Sorokin PB, Jin C, Ni J, et al. Large scale growth and characterization of atomic hexagonal boron nitride layers. Nano letters 2010;10(8):3209–15.
[19] Zhi C, Bando Y, Tang C, Kuwahara H, Golberg D. Large-scale fabrication of boron nitride nanosheets and their utilization in polymeric composites with improved thermal and mechanical properties. Adv Mater 2009;21(28):2889–93.
[20] Illy B, Shollock BA, MacManus-Driscoll JL, Ryan MP. Electrochemical growth of ZnO nanoplates. Nanotechnology 2005;16(2):320.
[21] Zhang L, Huang H. Young's moduli of ZnO nanoplates: Ab initio determinations. Appl Phys Lett 2006;89(18). 183111-183111.
[22] Tian ZR, Voigt JA, Liu J, Mckenzie B, Mcdermott MJ, Rodriguez MA, et al. Complex and oriented ZnO nanostructures. Nat Mater 2003;2(12):821–6.
[23] Wang YZ, Li FM. Dynamical properties of nanotubes with nonlocal continuum theory: a review. Sci China: Phys, Mech Astron 2012;55:1210–24.
[24] Wang CM, Zhang YY, Xiang Y, Reddy JN. Recent studies on buckling of carbon nanotubes. ASME Appl Mech Rev 2010;63:030804.
[25] Arash B, Wang Q. A review on the application of nonlocal elastic models in modeling of carbon nanotubes and graphenes. Comput Mater Sci 2012;51:303–13.
[26] Zhu Y, Murali S, Cai W, Li X, Suk JW, Potts JR, et al. Graphene and graphene oxide: synthesis, properties, and applications. Adv Mater 2010;22(35):3906–24.
[27] Zhang B, Cui T. An ultrasensitive and low-cost graphene sensor based on layer-by-layer nano self-assembly. Appl Phys Lett 2011;98(7). 073116-073116.
[28] Rogers GW, Liu JZ. Graphene actuators: quantum-mechanical and electrostatic double-layer effects. J Am Chem Soc 2011;133(28):10858–63.

[29] Potts JR, Dreyer DR, Bielawski CW, Ruoff RS. Graphene-based polymer nanocomposites. Polymer 2011;52(1):5–25.
[30] Pumera M. Graphene in biosensing. Mater Today 2011;14(7):308–15.
[31] Oniszczuk Z. Free transverse vibrations of an elastically connected rectangular simply supported double-plate complex system. J Sound Vib 2000;236(4):595–608.
[32] Hedrih KS. Dynamics of coupled systems. Nonlinear Anal: Hybrid Syst 2008;2(2):310–34.
[33] Wong EW, Sheehan PE, Lieber CM. Nanobeam mechanics: elasticity, strength, and toughness of nanorods and nanotubes. Science 1997;277(5334):1971–5.
[34] Cheng MN, Cheung CF, Lee WB, To S, Kong LB. Theoretical and experimental analysis of nano-surface generation in ultra-precision raster milling. Int J Mach Tools Manuf 2008;48(10):1090–102.
[35] Han TW, He PF, Wang J, Wu AH. Molecular dynamics simulation of a single graphene sheet under tension. Carbon 2011;49(1):353.
[36] Reddy CD, Rajendran S, Liew KM. Equilibrium configuration and continuum elastic properties of finite sized graphene. Nanotechnology 2006;17(3):864.
[37] Kitipornchai S, He XQ, Liew KM. Continuum model for the vibration of multilayered graphene sheets. Phys Rev B 2005;72(7):075443.
[38] He XQ, Kitipornchai S, Liew KM. Resonance analysis of multi-layered graphene sheets used as nanoscale resonators. Nanotechnology 2005;16(10):2086.
[39] Liew KM, He XQ, Kitipornchai S. Predicting nanovibration of multi-layered graphene sheets embedded in an elastic matrix. Acta Mater 2006;54(16):4229–36.
[40] Eringen AC. On differential equations of nonlocal elasticity and solutions of screw dislocation and surface waves. J Appl Phys 1983;54(9):4703–10.
[41] Shi JX, Ni QQ, Lei XW, Natsuki T. Nonlocal elasticity theory for the buckling of double-layer graphene nanoribbons based on a continuum model. Comput Mater Sci 2011;50(11):3085–90.
[42] Pradhan SC, Murmu T. Small scale effect on the buckling of single-layered graphene sheets under biaxial compression via nonlocal continuum mechanics. Comput Mater Sci 2009;47(1):268–74.
[43] Murmu T, Pradhan SC. Small-scale effect on the free in-plane vibration of nanoplates by nonlocal continuum model. Phys E: Low-dimensional Syst Nanostruct 2009;41(8):1628–33.
[44] Murmu T, Pradhan SC. Buckling of biaxially compressed orthotropic plates at small scales. Mech Res Commun 2009;36(8):933–8.
[45] Pradhan SC, Murmu T. Small scale effect on the buckling analysis of single-layered graphene sheet embedded in an elastic medium based on nonlocal plate theory. Phys E: Low-dimensional Syst Nanostruct 2010;42(5):1293–301.
[46] Ansari R, Sahmani S, Arash B. Nonlocal plate model for free vibrations of single-layered graphene sheets. Phys Lett A 2010;375(1):53–62.
[47] Shen L, Shen HS, Zhang CL. Nonlocal plate model for nonlinear vibration of single layer graphene sheets in thermal environments. Comput Mater Sci 2010;48(3):680–5.
[48] Ansari R, Rajabiehfard R, Arash B. Nonlocal finite element model for vibrations of embedded multi-layered graphene sheets. Comput Mater Sci 2010;49(4):831–8.
[49] Wang YZ, Li FM, Kishimoto K. Flexural wave propagation in double-layered nanoplates with small scale effects. J Appl Phys 2010;108(6). 064519-064519.
[50] Babaei H, Shahidi AR. Small-scale effects on the buckling of quadrilateral nanoplates based on nonlocal elasticity theory using the Galerkin method. Arch Appl Mech 2011;81(8):1051–62.
[51] Wang YZ, Li FM, Kishimoto K. Thermal effects on vibration properties of double-layered nanoplates at small scales. Compos Part B: Eng 2011;42(5):1311–7.
[52] Ansari R, Arash B, Rouhi H. Vibration characteristics of embedded multi-layered graphene sheets with different boundary conditions via nonlocal elasticity. Compos Struct 2011;93(9):2419–29.
[53] Malekzadeh P, Setoodeh AR, Alibeygi Beni A. Small scale effect on the free vibration of orthotropic arbitrary straight-sided quadrilateral nanoplates. Compos Struct 2011;93(7):1631–9.
[54] Narendar S, Gopalakrishnan S. Scale effects on buckling analysis of orthotropic nanoplates based on nonlocal two-variable refined plate theory. Acta Mech 2012;223(2):395–413.
[55] Kiani K. Vibrations of biaxially tensioned-embedded nanoplates for nanoparticle delivery. Ind J Sci Technol 2013;6(7):4894–902.
[56] Arani AG, Kolahchi R, Vossough H, Abdollahian M. Vibration and stability analysis of a Pasternak bonded double-GNR-system based on different nonlocal theories. J Solid Mech 2013;5(1):92–106.
[57] Lin Q, Rosenberg J, Chang D, Camacho R, Eichenfield M, Vahala KJ, et al. Coherent mixing of mechanical excitations in nano-optomechanical structures. Nat Photonics 2010;4(4):236–42.
[58] Liu M, Yin X, Zhang X. Double-layer graphene optical modulator. Nano letters 2012;12(3):1482–5.
[59] Gong L, Young RJ, Kinloch IA, Riaz I, Jalil R, Novoselov KS. Optimizing the reinforcement of polymer-based nanocomposites by graphene. ACS nano 2012;6(3):2086–95.
[60] Hu K, Kulkarni DD, Choi I, Tsukruk VV. Graphene–polymer nanocomposites for structural and functional applications. Progr Polym Sci 2014. http://dx.doi.org/10.1016/j.progpolymsci.2014.03.001.
[61] Kim H, Abdala AA, Macosko CW. Graphene/polymer nanocomposites. Macromolecules 2010;43(16):6515–30.
[62] Paul DR, Robeson LM. Polymer nanotechnology: nanocomposites. Polymer 2008;49(15):3187–204.
[63] Young RJ, Kinloch IA, Gong L, Novoselov KS. The mechanics of graphene nanocomposites: a review. Compos Sci Technol 2012;72(12):1459–76.
[64] Pradhan SC, Phadikar JK. Nonlocal elasticity theory for vibration of nanoplates. J Sound Vib 2009;325(1):206–23.
[65] Pradhan SC, Phadikar JK. Small scale effect on vibration of embedded multilayered graphene sheets based on nonlocal continuum models. Phys Lett A 2009;373(11):1062–9.
[66] Murmu T, Adhikari S. Nonlocal vibration of bonded double-nanoplate-systems. Compos Part B: Eng 2011;42(7):1901–11.
[67] Murmu T, Sienz J, Adhikari S, Arnold C. Nonlocal buckling behavior of bonded double-nanoplate-systems. J Appl Phys 2011;110(8). 084316-084316.
[68] Pouresmaeeli S, Fazelzadeh SA, Ghavanloo E. Exact solution for nonlocal vibration of double-orthotropic nanoplates embedded in elastic medium. Compos Part B: Eng 2012;43(8):3384–90.
[69] Murmu T, Sienz J, Adhikari S, Arnold C. Nonlocal buckling of double-nanoplate-systems under biaxial compression. Compos Part B: Eng 2013;44(1):84–94.
[70] Eringen AC, Edelen DGB. On nonlocal elasticity. Int J Eng Sci 1972;10:233–48.
[71] Reddy JN. Mechanics of laminated composite plates and shells: theory and analysis/JN Reddy. CRC press; 2004.
[72] Graff KF. Wave motion in elastic solids. New York: Dover Publications; 1975.
[73] Rašković D. On some characteristics of the frequency equation of torsional vibrations of light shafts with several disks. Public l'Inst Math 1953;V(05):155–64. http://elib.mi.sanu.ac.rs/files/journals/publ/11/16.pdf.
[74] Rašković D. Small forced damping vibrations of homogeneous torsional system with special static constraints. Public l'Inst Math 1963;3(13):27–34. http://elib.mi.sanu.ac.rs/files/journals/publ/23/3.pdf.
[75] Stojanović V, Kozić P, Janevski G. Exact closed-form solutions for the natural frequencies and stability of elastically connected multiple beam system using Timoshenko and high-order shear deformation theory. J Sound Vib 2013;332:563–76.
[76] Wang CY, Murmu T, Adhikari S. Mechanisms of nonlocal effect on the vibration of nanoplates. Appl Phys Lett 2011;98(15):153101–153101-3.